Session IV, Tuesday, June 20, morning

L11

X-RAY CHARACTERIZATION OF THIN LAYERS

L. Horák

Department of Condensed Matter Physics, Faculty of Mathematics and Physics
horak@karlov.mff.cuni.cz

A *layer* can be defined as a material of single thickness covering a surface of a different material (called substrate). On the other hand, the meaning of the word *thin* is quite ambiguous in exact thickness limit. However, from an X-ray methods standpoint, it is quite reasonable to consider the thickness to be much smaller than the absorption length of X-ray radiation in a material. There are two reasons: Firstly, the volume of such layers is so small that experimental setting has to be adjusted to enhance the measured signal. Secondly, the primary beam and the scattered beam has to transmit through the surface of the layer, which restricts the geometry of the experiment, in other words, crystal cannot be rotated to arbitrary position.

In the talk, we will give short overview of experimental setting, measurement and data evaluation of probably most common characterization techniques for thin layer. Firstly, the X-ray reflectivity is one of the exclusively surface techniques (for example see Figure 1). Since it is sensitive only to mean electron density in the sample, it can be successfully used for the study of amorphous, porous, polycrystalline, and even monocrystalline layers. It makes available information on the thickness of the layer, its relative density and the roughness of the surface and interfaces. It can be used not only for single layers, but it is powerful in determination of these parameters for the full stack of different sublayers. The maximal thickness is limited by the penetration depth that is quite low for low incident angle. On the other hand it can successfully detect a few nanometers thick oxide layer on the surface.

Polycrystalline thin layers as some coatings or active layers are usually studied using powder diffractometry in order to identify the crystallographic phases and other related parameters, e.g. grain sizes. Since the signal from the layer using usual Bragg-Brentano geometry is very weak, one has to use different geometry to enhance the layer signal. This can be achieved for instance using parallel beam geometry, in which the penetration depth is tuned by the angle of incidence (example in Figure 2).

Thirdly, very often characterizing experiment for epitaxial thins layers is the determination of the lattice relaxation state. Using Reciprocal space mapping, one can very easily see if the layer lattice is laterally adjusted to the substrate lateral periodicity (co called pseudomorphic layers) or it is (partially) relaxed, i.e. the layer unit cell is not (fully) distorted with respect to its bulk prototype. This information come out from the comparison of the substrate peak po-

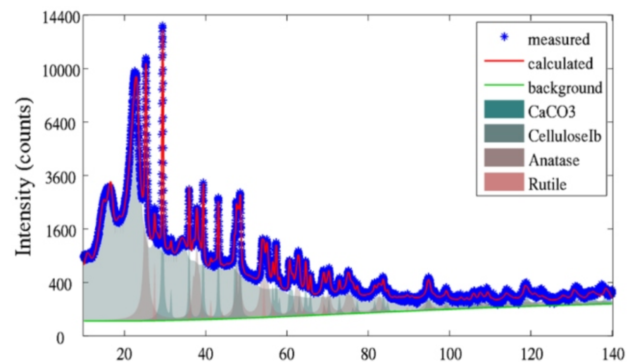

Figure 2. Standard powder pattern measured with fixed incidence angle to enhance the signal from the layer.

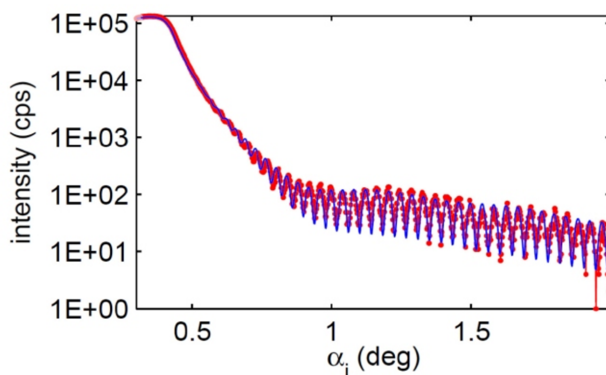

Figure 1. Example of measured reflectivity curve fitted by the simulation. The thickness can be determined from the frequency of the oscillations.

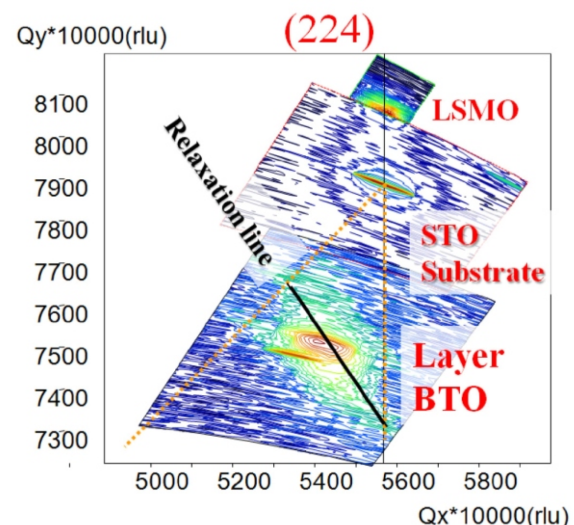

Figure 3. Reciprocal space map of asymmetric diffraction (224). The peak from pseudomorphic LSMO is located on the STO truncation rod, while the BTO peak is off this rod showing partial lattice relaxation.

sitions with those of the layer. Figure 3 shows the example of BTO thin layer partially relaxed on LSMO pseudomorphically grown on STO substrate.

Lastly, we will show quite challenging task to determine the structure of the monocrystalline layer including atomic positions. It is not so straightforward using structure refinement from standard powder or monocrystal diffractometry. The main obstacle is; that the signal from the substrate is usually much stronger and it is overlapped with the signal from the layer. However, using high resolution diffractometry we can distinct the presence of the signal from the layer. Nevertheless, the substrate signal has to be necessarily incorporated into the structure solution, since we measure the interference pattern of these two signals. For example see Figure 4 which shows the interference pattern measured along several crystal truncation rods.

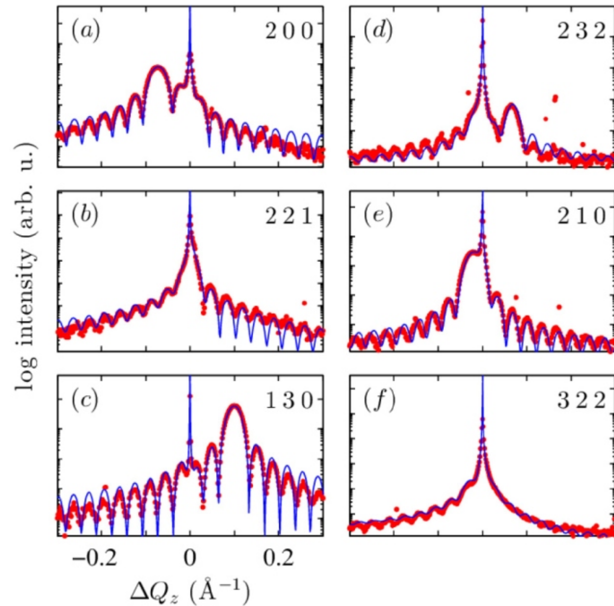

Figure 4. Measure intensity distribution along crystal truncation rods (red) is fitted by the simulation (blue). The interference between the wave diffracted in substrate and in the layer has to be taken into account.

L12

NEW NONSTANDARD MODELS IN MSTRUCT AND UNCONVENTIONAL ANALYSIS OF NANOCRYSTALLINE AND AMORPHOUS LIKE MATERIALS

Z. Matěj[1], M. Dopita[2], J. Endres[2]

[1]MAX IV Laboratory, Lund University, Lund, Sweden

[2]Faculty of Mathematics and Physics, Charles University, Praha, Czech Republic

zdenek.matej@maxiv.lu.se

Beside crystal structure solution, refinement of lattice parameters and quantitative phase analysis, characterization of sample microstructure from powder diffraction data is one of the most common quantitative crystallographic methods used in material science. There are numerous free crystallographic software available and one originally developed in Prague, called MSTRUCT [1-2], is just suitable for the microstructure analysis. Thanks to the original design based on ObjCryst/FOX [3] it is free and modular, i.e. various new microstructure models can be added by everyone with appropriate technical and scientific knowledge. An MSTRUCT extension for the line profile analysis of individual diffraction peaks and its application to materials with anisotropic line broadening were reported in [4] in 2014. In this contribution we describe new nonstandard models implemented and used for the diffraction analysis. These are:

- anisotropic size broadening from crystallites with rod, platelet and ellipsoidal shape [5]
- instrumental function for parallel beam reflection geometry with position sensitive detectors
- stacking faults on prismatic planes in Tungsten Carbide
- Warren-Bodenstein model for turbostratic nanoparticles [6]
- configuration model for description of bimodal microstructure [7]

Anisotropic size broadening

Anisotropic size broadening model was missing in MSTRUCT for a long time. A model of rods and platelets like crystallites [5] is briefly introduced and compared with result from the classical profile analysis [4]. Recently the models of shape broadening were also complemented with quite common model of ellipsoidal shape that is an independent contribution (*Jan Enders from Charles Uni.*).

Instrumental function for parallel beam reflection geometry with position sensitive detectors

Coplanar parallel beam geometry is often used for thin films measurements. With laboratory instruments it is optimally complemented with a long Soller slits analyser making the measurement directionally sensitive and providing a decent resolution (0.05° 0.3°). Nowadays linear posi-

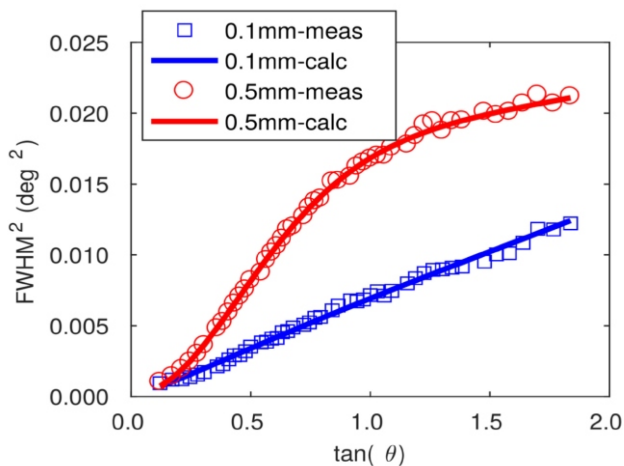

Figure 1. Angular dependence of FWHM of instrumental function measured on LaB_6 standard in the parallel beam geometry with area detector (diffraction beamline I711). Blue squares show the case of very small vertical incidence beam slit opening (0.1 mm) whereas red circles represent the case when diffracting sample area is relatively large (slit opening 0.5 mm). Fit with a specific model (lines).

tion sensitive and area detectors are very common in X-ray laboratories and micr focusing X-ray optics can deliver small beam to sample not only at synchrotrons. As already present the position sensitive detector can be an alternative to the setup with analyser under the favourable geometrical conditions (diffracting sample area, detector distance and strip or pixel dimensions). However when the diffracted sample area is still finite and in a common case of constant incidence beam angle, the resolution is dependent on the exit angle of the beam. We introduce an additional term describing this effect. A comparison is depicted in Fig. 1.

Stacking faults on prismatic planes in Tungsten Carbide

Stacking faults on prismatic {1-100} planes in hexagonal

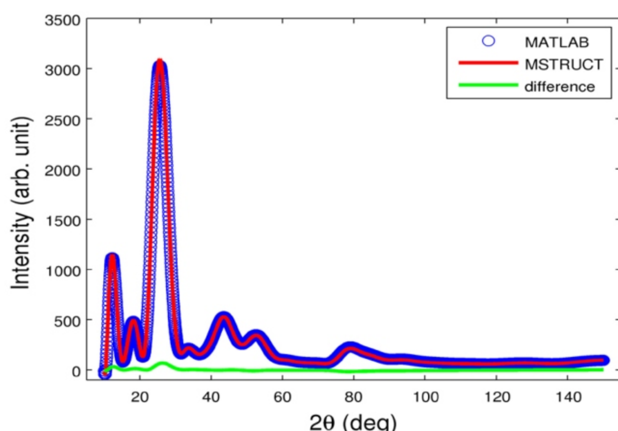

Figure 2. Comparison of original Warren-Bodenstein simulation of Carbon black nanoparticles as done in MATLAB [6] (blue points) and MSTRUCT implementation (red line). CuK wavelength.

WC are quite common defects. We present an alternative description of diffraction line broadening that is very similar to an educational example of 1D atomic chain for phonon dynamics. We compare the MSTRUCT implementation with DIFFaX simulations and experimental data.

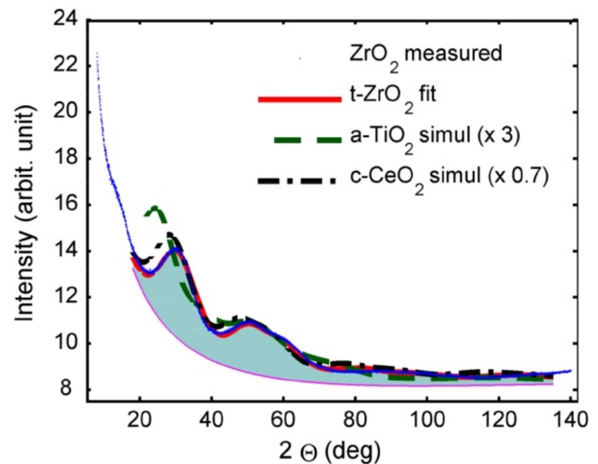

Figure 3. XRD pattern of ZrO_2 (blue points) from [8] and its fit (red curve) using a model of tetragonal-ZrO_2 crystalline domains of extremely small size (D ~ 0.8 nm). This corresponds to about 8 ZrO_2 molecules. For comparison similar simulated patters for anatase TiO_2 (green dash curve) and cubic CeO_2 (black dot-dash) are included. CuK wavelength.

Warren-Bodenstein model for turbostratic nanoparticles

Scattering from turbostratic (Carbon) nanoparticles can not be described by standard methods because of lack of orientation ordering of subsequent 2D Graphene-like layers. A Warren-Bodenstein method for a fast computation of this effect as used by Dopita et al. [6] was implemented (see Fig. 2) in order to quantitatively characterize samples of crystalline mixtures with Carbon black nanoparticles used as fillers.

Configuration model for description of bimodal microstructure

Uniform microstructure of a given crystalline phase is a common assumption in diffraction data analysis. However it is often not the case in nature. Bimodal grain size and the interaction between the two-microstructures with the same or very similar atomic structure is a key point driving properties of fine grained metals and alloys. Similar effects are crucial for catalytic nanoparticles, nucleation and crystallization processes or structural changes in pigments of ancient paintings. Refinement of bimodal microstructure of recrystallized fined grained Copper was discussed in [7]. It is also shown there the method is very robust for nanocrystalline metal oxides catalysts.

Unconventional analysis of nanocrystalline and amorphous like materials

Another very common case is that part of the sample is amorphous. Conventional diffraction analysis cannot give information about non-crystalline fraction of the sample. Pair distribution function measurement may be the solution. However in many cases, see Fig. 3, the sample state is often clear even from low energy (8-15 keV) or laboratory data. Fig. 3 illustrates diffraction patterns from such amorphous-like materials simulated by setting extremely small

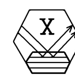

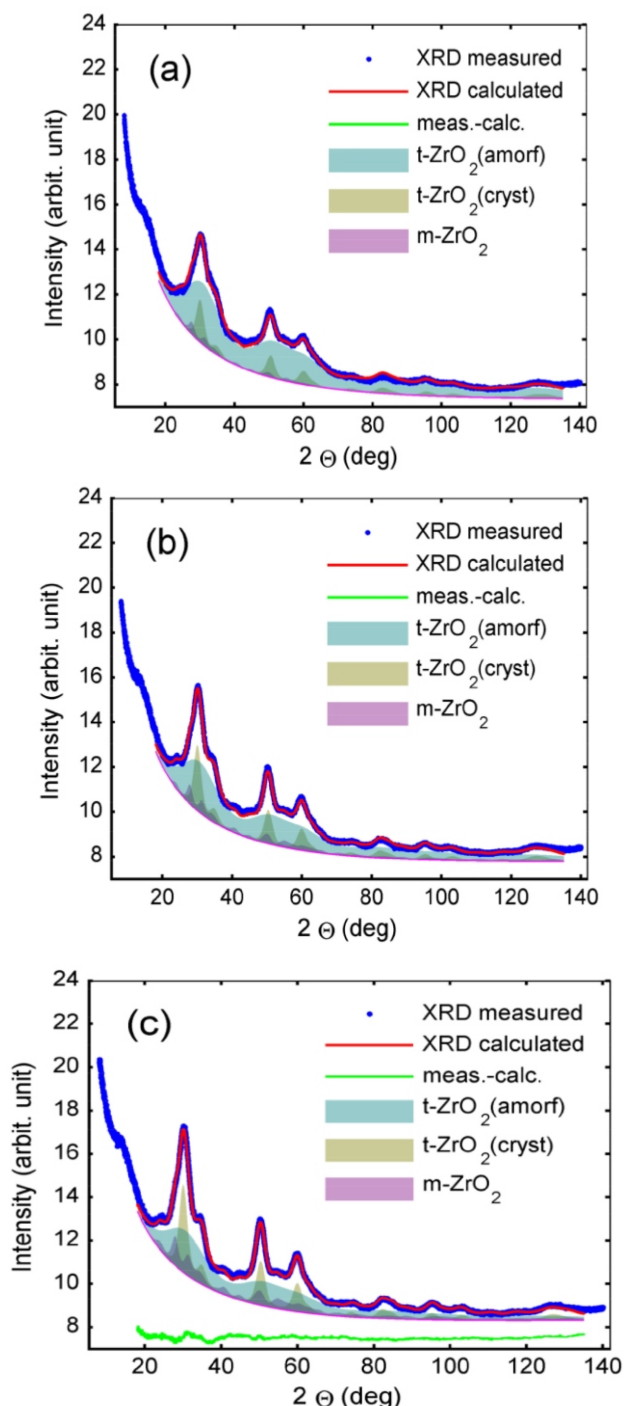

Figure 4. Pattern decomposition of multiphase ZrO_2 nanocrystalline samples prepared at different conditions [8]. Tetragonal t-ZrO_2 phase posses bimodal microstructure. Model assumes mixture of nanocrystalline t-ZrO_2 with crystallites size $D \sim 4$ nm and amorphous-like fraction similar to Fig. 3. It is evident that the amorphous-like contribution is changing with preparation conditions (differences between figures a-c). Whereas microstructure parameters related to tetragonal and monoclinic ZrO_2 crystalline phases do not vary so much, including relative weight fraction of crystalline t-ZrO_2 and m-ZrO_2. CuK wavelength.

crystallites size ($D \sim 0.8$ nm). In this case it also clearly evident which metal oxide (TiO_2, CeO_2, ZrO_2) is present in the sample. In spite of a good fit the phase can not be considered as crystalline as the potential crystal would consist only from about 8-12 molecules. Also the refined model (lattice) parameters can be subjected to systematic deviations [9].

Fig. 4 presents an application case when the amorphous-like oxide is present in the sample together with two additional crystalline phases. The amorphous content can be well characterised just from simple Rietveld refinement without any addition of internal reference standard and the nucleation process can be studied on the pure material.

1. Z. Matěj, R. Kužel, L. Nichtová, *Powder Diffr.*, **25** S2, (2010), 125. doi: 10.1154/1.3392371

2. Z. Matěj, R. Kužel, M. Dopita, *MSTRUCT*, www.xray.cz/mstruct (May 26, 2017).

3. V. Favre-Nicolin & R. Cerny, *J. Appl. Cryst.*, **35**, (2002), 734. doi: 10.1107/S00218898020

4. Z. Matěj, T. Brunátová, L. Matějová, V. Valeš, D. Popelková, R. Kužel, *Materials Structure in Chem. Bio. Phys. Tech.*, **21** no. 2, (2014), 91. url: goo.gl/Kxc4Uw

5. T. Brunatova, Z. Matej, P. Oleynikov, J. Vesely, S. Danis, D. Popelkova, R. Kuzel, *Mater. Characterization*, **98**, (2014), 26. doi: 10.1016/j.matchar.2014.10.008

6. M. Dopita, M. Emmel, A. Salomon, M. Rudolph, Z. Matěj, Ch.G. Aneziris, D. Rafaja, *Carbon*, **81**, (2015), 272. doi 10.1016/j.carbon.2014.09.058

7 Z. Matěj, A. Kadlecová, M. Janeček, L. Matějová, M. Dopita, R. Kužel, Powder Diffr., **29** S2, (2014), S35. doi: 10.1017/S0885715614000852

8. L. Matějová, Z. Matěj, *J. Supercritical Fluids*, Nanostructured ZrO_2 synthesized by using pressurized and supercritical fluids - its structural and microstructural evolution and thermal stability, *accepted*

9. I. Grey & N.C. Wilson, J. Solid State. Chem., **180**, (2007), 670. doi: 10.1016/j.jssc.2006.11.028

The authors thank MAX IV Laboratory (Lund, Sweden) and ID22, ESRF (Grenoble, France) for providing the beamtime.